

METAMORPHISM AND FISSION-TRACK AGE DETERMINATION OF APATITE CRYSTALS FROM DEMİRCİ-BORLU REGION, GÖRDES SUBMASSIF OF THE MENDERES MASSIF-WESTERN TURKEY

Osman CANDAN*; Cahit HELVACI*; G. BÖHLER**; G. WALDER** and T.D. MARK**

ABSTRACT. - Investigated area is located in the Gördes submassif of the Menderes massif, the metamorphic basement consists of the following lithologies in ascending order: Sillimanite-gamet gneiss. sillimanite-gamet-kyanite schist. sillimanite-staurolite-gamet-kyanite schist, staurolite-garnet schist and garnet mica schist. Kyanite-andalusite pegmatoids which occur within the kyanite-bearing schists were formed in the course of the last major metamorphism giving the final stage to the Menderes massif. The metamorphic basement is overlain by the allochthonous units which are relicts of the Lycian nappes which caused the last major metamorphism during the Eocene-Oligocene time in Menderes massif. The age of the apatite crystals obtained from the pegmatoids arc determined by the fission-track method. The cooling age of the apatite crystals ranging from the Early Oligocene to Early Miocene are in good agreement with the field observations in the study area and geological evidences relating to the Menderes massif.

INTRODUCTION

Menderes massif is a large area of metamorphic rocks lying in the western part of Turkey. The study area is approximately 200 km northeast of İzmir city (Fig. 1). Although investigations on the Menderes massif have continued since the pioneering work of Phillipson (1911), the polyphase history and timing the metamorphic events within the basement remain unclear. This paper provides new petrological and age date to the PT(t) pathways of the schists.

In particular, we report fission-track age determinations on apatites from the pegmatoids within the kyanite-schists from the northern part of the Menderes massif. We have also attempted to interpret previous geologic and radiometric studies of the Menderes massif in the light of our investigations.

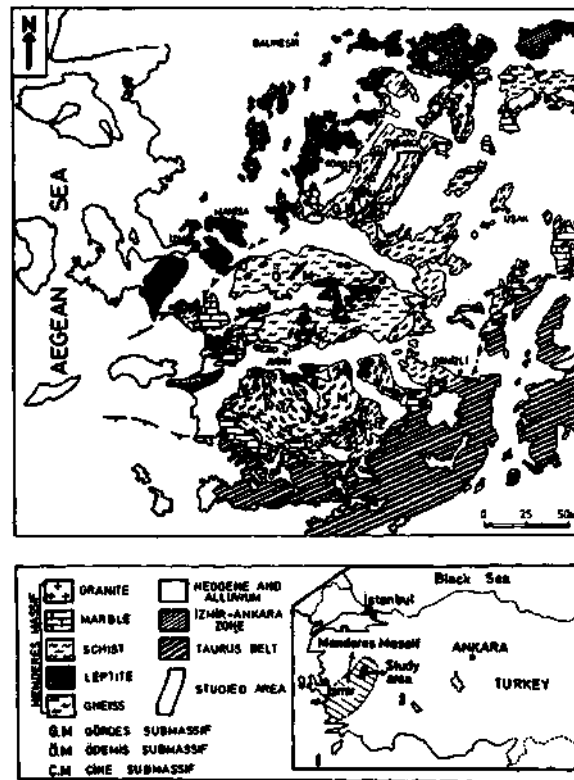


Fig. 1 - Location map of the study area (Candan, 1988).

GEOLOGICAL SETTING OF THE REGION

Although considerable areas of the Menderes massif have now been mapped in detail and studied by several workers, problems still to be solved include the depositional ages of the core and cover rock units of the massif, the metamorphic phases affecting these rock units, and the ages of the metamorphism. There are some different opinions on these subjects.

Menteşe marbles, which contain emery deposits, occur at the southern boundary of the Menderes massif and the Göktepe formations which overlie these marbles, were deposited in Permian time as suggested by Önay (1949), Kaaden and Metz (1954) and Schuiling (1962). The same authors suggested that these formations were metamorphosed during the Hercynian orogeny. Akdeniz et al. (1980) and Akdeniz and Konak (1979) argue that the protoliths for the metamorphic sequence are Precambrian-Paleozoic in age, and they are overlain by unmetamorphosed Triassic-Upper Cretaceous rock units with an angular unconformity. They also suggested that the metamorphism took place during the Hercynian orogeny.

On the other hand, Brinkmann (1966, 1967) suggested that the core of the Menderes massif was metamorphosed in Late Precambrian-Early Cambrian time. The same author also argued that the cover rock units of the sequence in the massif continued until Early Jurassic times, and were metamorphosed during Middle Jurassic times. According to Wippem (1964), the cover rock units and the overlying Göktepe formation are Devonian and Permo-Carboniferous in age respectively, whereas the emery bearing marbles are probably Triassic in age. Wippem (1964) also noted that the age of the metamorphism is Jurassic. Another opinion widely accepted presently on the major metamorphism of the Menderes massif will be treated in detail in the following sections.

LITHOSTRATIGRAPHY

On the basis of field observations and petrographic studies, the rocks in the study area can be divided into three main groups: Metamorphic units of the Menderes massif, allochthonous units overlying the metamorphic basement with tectonic contacts, and Neogene volcanic and sedimentary rocks resting on both metamorphic and allochthonous units with an angular unconformity (Fig. 2).

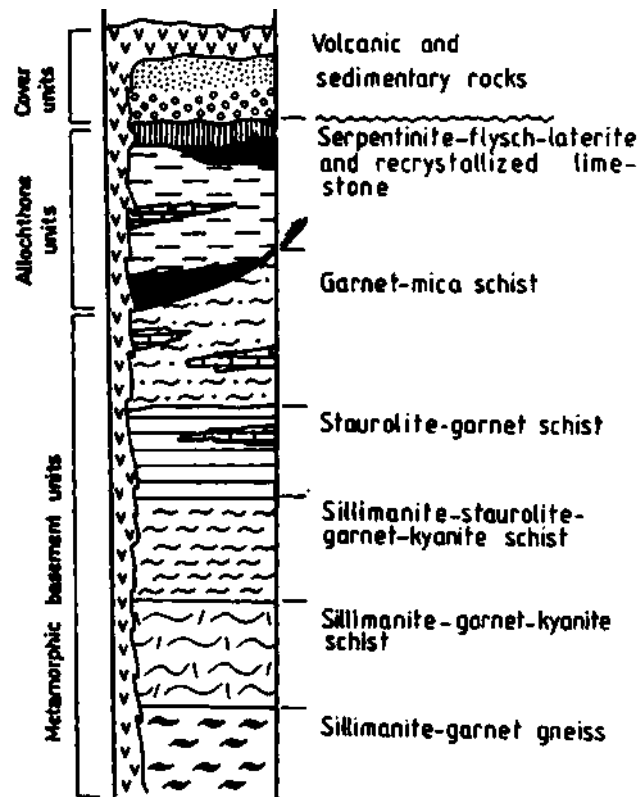


Fig. 2 - Generalized columnar section of the study area (Candan, 1988).

In the region, the metamorphic sequence consists of the following successions in ascending order Sillimanite-gamet gneiss; sillimanite-garnet-kyanite schist; sillimanite-staurolite-gamet-kyanite schist with abundant kyanite-andalusite pegmatoids; staurolite-garnet schist and garnet-mica schist with marble intercalations containing emery deposits. The units and the main mineral assemblages observed in these rocks are shown on Figure 3.

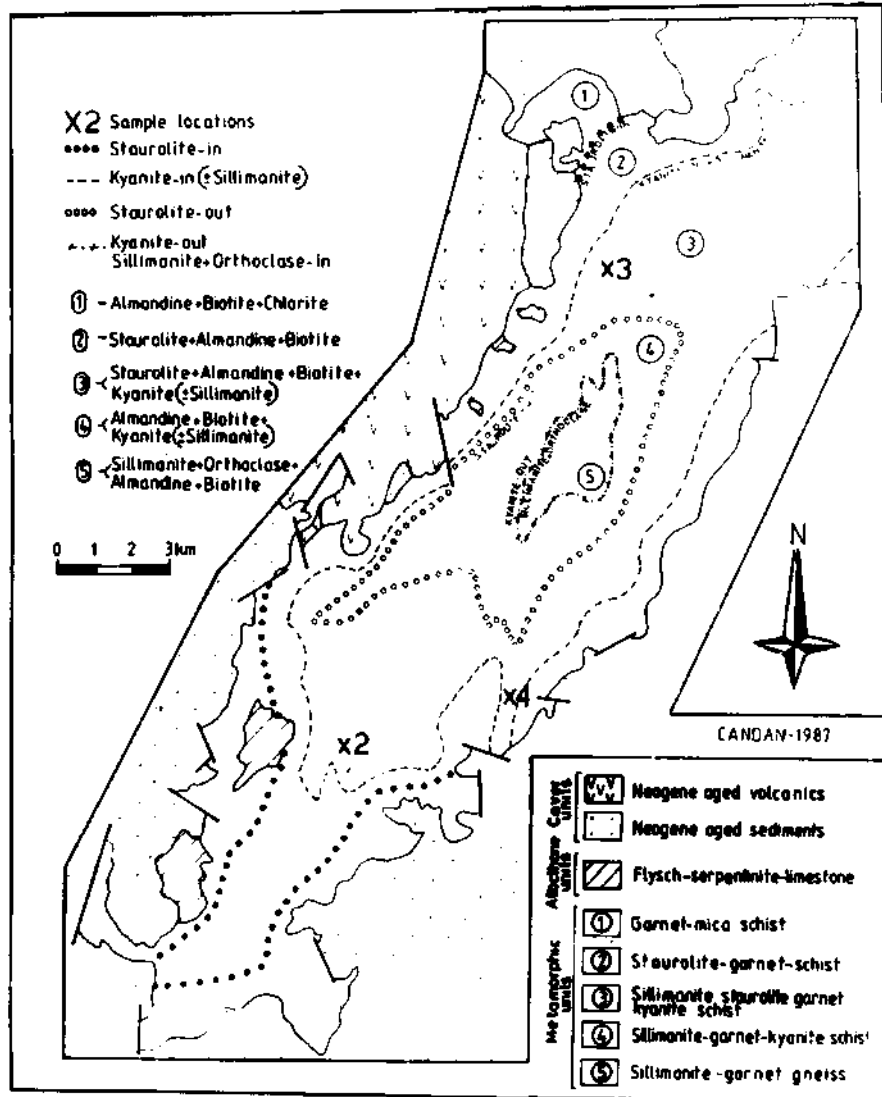


Fig. 3 - Main units and stable mineral assemblages observed within these rocks, and the isograd map of the study area (simplified from Candan, 1988).

The allochthonous units were emplaced over the metamorphic basement units along nearly horizontal thrust planes and occur as klippe on the metamorphic rocks. The allochthonous units consist mainly of limestone, conglomerate, sandstone, shale and ophiolitic rocks. Large recrystallized muscovite and chlorite crystals are observed within deformed pelites. These new minerals were formed in the course of the emplacement of the allochthonous units. Other rock types identified within the allochthonous units are harzburgite, which is often totally altered to serpentinite, recrystallized limestone and pink-coloured thin-bedded limestone. Lateritic soils are commonly developed above mentioned ultrabasic rocks. According to Dürr (1975), Dürr et al. (1978) and Şengör et al. (1984), these allochthonous units are relicts of the Lycian nappes which were transformed from the north to the south on the Menderes massif during the Eocene-Oligocene time.

Middle Miocene rock units consisting of volcanic and volcano-sedimentary rocks rest on both metamorphic and allochthonous units with angular unconformity.

PETROGRAPHY OF THE METAMORPHICS

Sillimanite-garnet gneiss

These rocks are the lowest rock units observed in the sequence and are composed of the following mineral assemblages: quartz+plagioclase+orthoclase+biotite+muscovite±sillimanite+garnet±chlorite+apatite+tourmaline and zircon. These rocks show mortar texture and contain fibrolitic sillimanites forming at the feldspar boundaries.

Kyanite-bearing schists

These rocks are widely distributed and can be divided into two subgroups according to their mineral composition as either sillimanite-garnet-kyanite schist or sillimanite-staurolite-garnet-kyanite schist. These schists have kyanite, staurolite and garnet porphyroblasts reaching up to 7-8 cm in size (Fig. 4).



Fig. 4 - Staurolite and kyanite crystals reaching up to 7-8 cm in size observed in the sillimanite-staurolite-garnet-kyanite schists. Stau-staurolite; ky-kyanite.

The mineral assemblage of the sillimanite - garnet - kyanite schists is quartz + plagioclase (An 27 - 30) + kyanite ± sillimanite + garnet + biotite + muscovite ± chlorite + apatite + zircon + tourmaline and sphene. Sillimanites are grouped in two different types according to their formation. The most abundant type is fibrolitic sillimanite growing between two feldspar boundaries, and the other is the polymorphic transformations from kyanite as a result of temperature increase during progressive metamorphism (Fig. 5). Garnets are represented by almandine ($Alm_{77}Prp_{19}Grs_4$), and all the chlorites in these rocks were formed after biotite by the last retrograde metamorphism.

The second group of the kyanite-bearing schists consist of quartz+plagioclase (An 23-25) ± sillimanite + kyanite ± andalusite + staurolite + garnet + biotite + muscovite ± chlorite+apatite + zircon + tourmaline and sphene. These rocks also contain staurolite and andalusite in contrast to the other kyanite-bearing schists. The staurolite porphyroblasts are extremely fractured and altered to chlorite and sericite.

Although all the Al_2SiO_5 polymorphs (kyanite-andalusite-sillimanite) exist in these schists, the petrographical observations and textural evidences suggested that these polymorphs are not in equilibrium. The polymorphic transformations from kyanite to sillimanite and andalusite due to increasing temperature and decreasing pressure respectively, are very common.



Fig. 5 - Polymorphic transformation from kyanite to sillimanite as a results of increasing temperature during the progressive metamorphism. Plane polarized light, 10 x. Sil-sillimanite; Ky-kyanite.

Kyanite-andalusite pegmatoids

Kyanite-andalusite pegmatoids reaching up to 10-12 m in size occur within the kyanite-bearing schists. These pegmatoids are often lens shaped and parallel to the schistosity (Fig. 6). The pegmatoids do not show internal zoning, and are enclosed by a biotite-rich envelope.

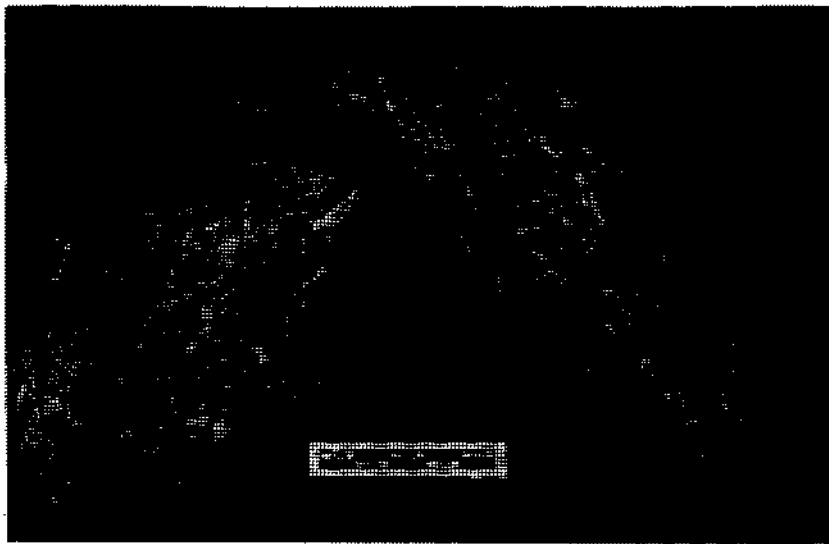


Fig. 6 - General appearance of kyanite-andalusite pegmatoids.

The general mineral assemblage of the pegmatoids is composed of quartz+plagioclase (An 6) + kyanite ± sillimanite + andalusite ± staurolite ± garnet + biotite + muscovite ± chlorite + apatite + zircon ± graphite + rutile and diaspore. The most abundant mineral of the pegmatoids is kyanite which occurs often in white, pale-blue, dark-blue and green colours and is often deformed.

The second most abundant mineral is dark pink andalusite altered widely to sericite. These minerals are formed after kyanite by polymorphic transformation (Fig. 7). Trace amounts of sillimanite are also formed after kyanite due to increasing temperature.

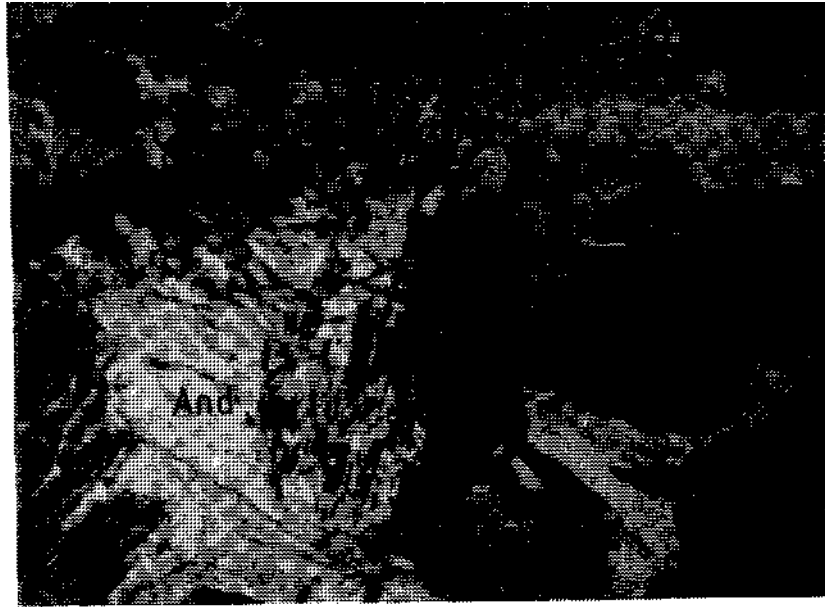


Fig. 7 - Polymorphic transformation from kyanite to andalusite in kyanite-andalusite, pegmatoids. Cross polar, 4x. and-andalusite; ky-kyanite.

Idiomorphic Fe-staurolite and garnet ($\text{Alm}_{76}\text{Prp}_{22}\text{Gr}_{22}$) are also important phases in the pegmatoids and occur with biotite, muscovite and chlorite (ripidolite and pycnochlorite) after biotite. The other important mineral of pegmatoids is pale green apatite with crystals often reaching 0.5 to 1 cm and rarely 7 to 8 cm in size (Fig. 8). Optic and diffractometric observa-



Fig. 8 - Euhedral apatite crystals intergrowing with kyanites in kyanite-andalusite pegmatoids. Ap-apatite.

tions indicate that these apatites are fluor-apatite which shows intergrowth with kyanite, and extend parallel to the mineral lineation of the wallrocks. These observations suggest that the crystallization of the apatites are synmetamorphic. For this reason the apatites are used to determine the age of the last main metamorphic phase affecting the Menderes massif.

Kyanite-andalusite pegmatoids were formed by the lateral migration of some elements, such as Al, Si, K, etc. from the wallrock of the Al-rich kyanite schists during the high-grade regional metamorphism affecting the region. The occurrence of the kyanite-andalusite pegmatoids only within the kyanite-bearing schists indicates that element migration took place for only short distances (Candan ve Dora, 1984; Candan, 1988). The large and pure kyanite crystals reaching up to 50-60 weight percentage in some pegmatoids are of economic importance. These rocks widely exploding are utilized as the raw material of the refractory industries.

Staurolite-garnet schist

Sillimanite-staurolite-garnet kyanite schists are overlain by the staurolite-garnet schists. These schists consist of mainly quartz + plagioclase + biotite + muscovite + staurolite + garnet + apatite + zircon, and they often alternate with muscovite-quartz schist and marbles containing emery deposits.

Garnet-mica schist

These rocks alternating with marble and muscovite-quartz schist in the region form the highest level of the metamorphic sequence in the region, and contain mainly quartz + plagioclase + biotite + muscovite + chlorite + garnet and zircon.

EXPERIMENTAL RESULTS

The basic theory and the experimental technique of fission-track dating has been reviewed up to 1975 by Fleischer et al. (1975). Certain points pertinent to the present determination are summarized in the following.

As fission-tracks in minerals become partly annealed under the influence of increased temperature, it is necessary to correct the uncorrected fission-track age formula. One method of correction is based on the observation that as a mineral sample is heated, the fission-track lengths decrease at a rate related to the track density decrease. The corrected fission-track age for apatite is given according to Mark et al. (1973) by

$$t_{1\min} = \frac{1}{\lambda_{\alpha}} \ln \left(1 + \frac{\lambda_{\alpha} \cdot \sigma_f \cdot I \cdot n}{\lambda_f} \cdot \frac{P_s}{P_i} \cdot K \right) \quad (1)$$

or

$$t_{1\min} = \frac{\sigma_f \cdot I \cdot n}{\lambda_f} \cdot \frac{P_s}{P_i} \cdot K \quad (2)$$

(for $t < 3 \times 10^8$ a)

The symbols have the following meanings: λ_{α} $1.54 \times 10^{-10} \text{ a}^{-1}$ time constant for the α -decay of ^{238}U (Spadavecchia and Hahn, 1967), λ_f $0.84 \times 10^{-16} \text{ a}^{-1}$ time constant for spontaneous fission of ^{238}U (Spadavecchia and Hahn, 1967), σ_f 582 barn induced fission cross section of ^{235}U by thermal neutrons (Hanna et al. 1968), I : 7.26×10^{-3} isotope abundance

ratio $^{235}\text{U}/^{238}\text{U}$ (De Wet and Turkstra, 1968), n integrated neutron flux. P_s and P_i measured area densities of spontaneous and induced fission-tracks, K correction factor with $K: l_i/l_s$ in apatite (Mark et al., 1973), l_i/l_s ration of average length of induced and spontaneous fission-tracks.

Mark et al. (1973) have shown that this corrected age $t_{l_{\min}}$ is the amount of the necessary to reduce the length of fission (produced in full length) by geothermal annealing to l_{\min} is the minimum track length-horizontal projection-which can be observed in the microscope; in apatite 2 mm). In other words, $t_{l_{\min}}$ is the age of tracks with the shortest length that can be detected today. If the track length ratio K is omitted in equ. (1) or (2), i.e. if $K: l_i/l_s$ is set equal to 1, a value of t is obtained called uncorrected fission-track age.

Following Mark et al. (1973, 1981 *a,b*) and Mark and Mark (1982) it is possible to determine by means of a theoretical calculation a temperature value, $T_{l_{\min}}$ corresponding to the measured and corrected fission-track age, $t_{l_{\min}}$ assuming a linear or exponential cooling rate. This calculated relationship is given Mark et al. (1981 *a,b*) and Mark and Mark (1982) and can be used to obtain a complete temperature-age determination (see also the discussion by Bertagnolli et al., 1981).

The preparation of the present apatite samples was done in the usual way (Koark et al., 1978). The track densities were counted with a texture analyzing system of Leitz combined with a phasecontrast Leitz Orthoplan microscope. In order to evaluate the reliability of the present determination (measurement of neutron flux etc.) a Durango apatite sample was measured simultaneously with the present apatite samples, yielding a value in excellent agreement with previous high precision determinations (Mark et al., 1981b).

Table 1 gives the present results of the counted track densities (the induced tracks were obtained by irradiating the annealed samples with a thermal neutron dose n of 9.36×10^{14} n/cm²) and track length ratios. Also shown in Table 1 are the determined corrected fission-track ages and the corresponding temperatures. It is interesting to note that these age determinations were confirmed by an additional independent measurement in our laboratory, yielding the values of 21, 27 and 35 my, respectively. We have also determined the uranium concentration (using the fission-track method described by Mark et al., 1974), yielding uranium concentrations of 22.5, 41.5 and 26 ppm for the samples A2, A3 and A4, respectively.

Table 1 - Experimental fission-track results for apatite crystals from the Menderes massif

Sample number	Uranium concentration in ppm	Absolute number of counted tracks		Fission-track areal densities in $10^5/\text{cm}^2$		P_s/P_i	$\overline{l_i/l_s}$	$t_{l_{\min}}$ in 10^6 a	$T_{l_{\min}}$ in °C
		spontaneous	induced	spontaneous	induced				
A2	22.5 ± 5	410	1214	2.1 ± 0.1	4.7 ± 0.15	0.45 ± 0.04	1.09 ± 0.5	23 ± 5	165
A3	41.5 ± 10	1051	1544	5.4 ± 0.2	7.9 ± 0.2	0.68 ± 0.05	1.16 ± 0.08	37 ± 7	163
A4	26 ± 5	678	1380	3.5 ± 0.15	5.3 ± 0.15	0.66 ± 0.06	1.18 ± 0.07	36 ± 7	163

CONCLUSIONS

The sedimentation in the Menderes massif continued until the beginning of Tertiary is now widely accepted, although previous workers had suggested Jurassic time for the upper limit of the sequence of the Menderes massif. According to Çağlayan et al. (1980), the sedimentation reaches to Upper Paleocene time, and as result of paleontological evidence, the emery-bearing marbles range from Triassic to Upper Cretaceous in age. The red marbles overlying the emery-bearing marbles are Upper Paleocene in age, whereas the same red coloured marbles are Eocene in age according to Gutnic et al. (1979). Dürr et al. (1978) suggested that the sedimentation in the Menderes massif continued until the Lower Tertiary time, and the main Harrovian metamorphism reached up to migmatization grade and took place during Eocene times.

Andriessen et al. (1979) subdivides three major metamorphic phases according to their radiometric studies by using K-Ar method on the emery-bearing series of the Menderes massif in Naxos island. The medium pressure/high temperature type metamorphism reaching up to anatexitic stage gives an age of 25 ± 5 my (Oligocene - Early Miocene). Şengör et al. (1984) and Akkök et al. (1984) also suggested that the age of the sequence in the Menderes massif reaches up to Eocene, and the main metamorphic phase is in between Eocene-Oligocene. This result coincidences with the radiometric age of 35 ± 5 my. This main metamorphism of the Menderes massif was a product of the latest Paleocene collision across Neo-Tethys and the consequent internal imbrication of the Menderes-Taurus blok that resulted in the burial of the Menderes massif area beneath the Lycian nappe complex (Şengör et al., 1984).

In summary, there are three main opinions regarding the age of the major metamorphism which affected the Menderes massif: Hercynian (Önay, 1949; Kaaden and Metz, 1954; Schuiling, 1962; Akdeniz and Konak, 1979), Middle Jurassic (Brinkmann, 1966, 1967; Wippert, 1964), and Eocene-Oligocene (Andriessen et al., 1979; Şengör et al., 1984; Akkök et al., 1984) in age as mentioned in the previous works.

As far as metamorphic paragenesis is concerned, the study area located in the northern part of the Menderes massif shows similarity to the Ödemiş submassif. In addition to this similarity, the presence of the emery bearing marbles interlayered with the schists in the region can be clearly correlated with the schists of the southern limb of the Menderes massif.

In the petrography section, it is already mentioned that the kyanite-andalusite pegmatoids were formed by the lateral migration of some elements from the wallrocks of the kyanite schists during the high-grade regional metamorphism that affected the region. Thus, the kyanite-andalusite pegmatoids were formed penecontemporaneously with the kyanite schists; which resulted from the major metamorphism giving the present appearance of the massif.

Apatite crystals intergrowing with kyanites can give the formation age of the schists. The experimental fission-track results for apatite crystals are shown in Table 1. As it is understood from these data that these cooling ages range between Early Oligocene and Early Miocene. These results are in good agreement with the geological evidence in Turkey and the radiometric age determination obtained from the Greek islands (Andriessen et al., 1979).

In the study area, the allochthonous units consisting of serpentinite, flysch and limestones, rest on the metamorphic basement with tectonic contacts. These allochthonous units are relicts of the Lycian nappes which caused the last major metamorphism during the Eocene-Oligocene time. These geological interpretations support the radiometric cooling ages obtained from the apatite crystals. Şengör et al. (1984) suggest that the final major metamorphism of the Menderes massif is completed during Middle Eocene-Early Oligocene, and the uplifting and cooling of the massif took place between Late Oligocene and Early Miocene with respect to the geotectonic evolution of the Western Anatolia. The obtained cooling ages ranging between Early Oligocene and Early Miocene of the apatite crystals from the study area are in good agreement with above mentioned concept of the cooling and uplifting stages which took place after the last major metamorphism of the massif.

Manuscript received September 26, 1989

REFERENCES

- Akdeniz, N. and Konak, N., 1979, Menderes Masifinin Simav dolayındaki kaya birimlerinin ve metabazik, metaultrabazik kayaların konumlan: Türkiye Jeol. Kur. Bull., 22, 175-183.
- ;— and Armağan, E., 1980, Akhisar (Manisa) güneydoğusundaki Alt Mesozoik kaya birimleri: Türkiye Jeol. Kur. Bull., 2, 77-90.
- Akkök, R.; Satır, M. and Şengör, C., 1984, Menderes masifinde tektonik olayların zamanlaması ve sonuçları: Ketin Sempozyumu Bildiri Özetleri, 93-94.
- Andriessen, P.A.M.; Boelrijk, N.A.I.M.; Hebeda, E.H.; Priem, H.N.A.; Verdurmen, E.A. Th and Verschure, R.H., 1979, Dating the events of metamorphism and granitic magmatism in the Alpine Orogen of Naxos (Cyclades, Greece): Contrib. Mineral. Petrol. 09, 215-225.
- Bertognolli, R.; Mark, E.; Bertel, E.; Pahl, M. and Mark, T.D., 1981, Determination of paleotemperatures of apatite with the fission-track method: Nucl. Tracks., 5, 175-180.
- Brinkmann, R., 1966, Geotektonische Gliederung von Westanatolien: N. Jb. Geol. Pal. Mh. 603-608.

- Brinkmann, R., 1967, Die Sudflanke des Menderes-Massive bei Milas, Bodrum und Ören: *Scien. Rep. Fac. Scien. Ege Univ.* 43,12 p.
- Candan, O., 1988, Demirci-Borlu arasında kalan yörenin (Menderes masifi kuzey-kanadı) petrografisi, petrolojisi ve mineralojisi: Doktora tezi, Dokuz Eylül Üniv. Müh. Mim. Fak. (unpublished).
- and Dora, O.Ö., 1984, Ahmetler-Üşümüş (Manisa) dolayında Menderes masifi metamorfizminin jeolojik incelemesi ve distenli pegmatoidlerin oluşumu: *Türkiye Jeol. Kur. Bull.*, 27, 45-58.
- Çağlayan, A.; Öztürk, M.; Öztürk, Z.; Sav, H. and Akat, U., 1980, Menderes masifi güneyine ait bulgular ve yapısal yorum: *Jeoloji Mühendisliği*, 10,7-19.
- De Wet, WJ. and Turkstra, J., 1968, Determination of Uranium-235 / Uranium-238 ratios by activation analysis utilizing high resolution d-spectrometry: *J. Radional. Chem.* 1,379-387.
- Dürr, S., 1975, Über Alter und geotektonische Stellung des Menderes-Kristallins / SW-Anatolian und seine equivalente in der Mittleren Aegaeis: *Marburg / Lahn, 1975, Federal Republic of Germany (These)*.
- ; Altherr, R.; Kellers, S.; Okrusch, M. and Seidel, E., 1978, The Median Aegean Crystalline belt, stratigraphy, suturcture, metamorphism, magmatism: *I.U.C.G. Sci. Rep.* 38,455-477.
- Fleischer, R.L.; Price, P.B. and Walker, R.M., 1975, Nuclear tracks in solids: Univ. California Press, Berkely. 1-605.
- Gutnic, M.; Monod, O.; Poisson, A. and Dumont, F., 1979, Géologie des Taurides Occidentales (Turquie): *Mem. Soc. Geol. Fr.* 58,109.
- Hanna, G.C.; Westcott, C.H.; Lemmel, H.D.; Leonard, B.R.; Story, J.J. and Attree, P.M., 1968, Revision of values for the 2200 m/s neutral constants for four fissile nuclides: *At. Energ. Rev.* 7, 3-29.
- Kaaden, G.V.D. and Metz, K., 1954, Datça-Muğla-Dalaman Çayı (GB Anadolu) arasındaki bölgenin jeolojisi: *Türkiye Jeol. Kur. Bull.*, 5, 1-2.
- Koark, H.J.; Mark, T.D.; Pahl, M.; Purtscheller, F. and Vartaian, R., 1978, Precambrian fission-track ages of sphene from the Caledonides of Mount Areskutan, Sweden: *Bull. Geol. Inst. Univ. Uppsala*, 7,103-108.
- Mark, E.; Pahl, M.; Purtscheller, F. and Mark, T.D., 1973, Thermische Ausheilung von Uran-Spatispuren in Apatiten. Alterskorrekturen und Beitrage zur geothermon chronologie: *Techemals. Mineral. Petr. Mitt.*, 20,131-154.
- ; ——; —— and ——, 1974, Comparative determination of uranium content by the fission-track method and by delayed neutrons: *Acta. Phys. Austr.* 40,261-271.
- ; and Mark, T.D., 1982, Solid state nuclear track detectors: Eds. P.H. Fowler and V.M., Clapham, Pergamon Press, Oxford, 389-394.
- Mark, T.D.; Vartanian, R.; Purtscheller, F. and Pahl, M., 1981 *a*, Fission-track annealing and application to the dating of Austrian sphene: *Acta. Puhs Austria*, 53,45-59.
- ; Pahl, M. and Vartanian, R., 1981 *b*, Fission-track annealing and fission-track age/temperature relationship in sphene: *Nuclear Tecnology*, 52,295-305.
- Önay, T., 1949, Über die Schmirgelgesteine SW-Anatoliens: *Schw. Min. Petr. Mitt. Bd.* 29, 359-491.
- Phillipson, A., 1911, Reisen und Forschungen in Westlishen Kleinasien: *Pet. Mitt. Erg. Heft.* 167-187, Gotha.
- Schuiling, R., 1962, Türkiye'ningüneybatısındaki Menderes Migmatitkompleksinin petrolojisi, yaşı ve yapısı hakkında: *MTA Bull.*, 58,71-84.
- Şengör, C; Satır, M. and Akkök, R., 1984, Timing of tectonic events in the Menderes Massif, Western Turkey: Implications for tectonic evolution and evidence for Pan-African basement in Turkey: *Tectonics*, 3, 7,693-707.
- Spadavewhia, A. and Hahn, B., 1967, Die Rotationskammer und einige Anwen dungen: *Helv. Phys. Acta*, 40, 1063-1079.